

# Host galaxies of long gamma-ray bursts in the *Millennium Simulation*

N. E. Chisari<sup>1</sup>\*, P. B. Tissera<sup>1,2</sup> and L. J. Pellizza<sup>1,2</sup>

<sup>1</sup> Instituto de Astronomía y Física del Espacio, Casilla de Correo 67, Suc. 28, 1428, Buenos Aires, Argentina

<sup>2</sup> Consejo Nacional de Investigaciones Científicas y Técnicas, CONICET, Argentina

submitted 2009 November 24, accepted 2010 June 09

## ABSTRACT

In this work, we investigate the nature of the host galaxies of long Gamma-Ray bursts (LGRBs) using a galaxy catalogue constructed from the *Millennium Simulation*. We developed a LGRB synthetic model based on the hypothesis that these events originate at the end of the life of massive stars following the collapsar model, with the possibility of including a constraint on the metallicity of the progenitor star. A complete observability pipeline was designed to calculate a probability estimation for a galaxy to be observationally identified as a host for LGRBs detected by present observational facilities. This new tool allows us to build an observable host galaxy catalogue which is required to reproduce the current stellar mass distribution of observed hosts. This observability pipeline predicts that the minimum mass for the progenitor stars should be  $\sim 75 M_{\odot}$  in order to be able to reproduce BATSE observations. Systems in our observable catalogue are able to reproduce the observed properties of host galaxies, namely stellar masses, colours, luminosity, star formation activity and metallicities as a function of redshift. At  $z > 2$ , our model predicts that the observable host galaxies would be very similar to the global galaxy population. We found that  $\sim 88$  per cent of the observable host galaxies with mean gas metallicity lower than  $0.6 Z_{\odot}$  have stellar masses in the range  $10^{8.5} - 10^{10.3} M_{\odot}$  in excellent agreement with observations. Interestingly, in our model observable host galaxies remain mainly within this mass range regardless of redshift, since lower stellar mass systems would have a low probability of being observed while more massive ones would be too metal-rich. Observable host galaxies are predicted to preferentially inhabit dark matter haloes in the range  $10^{11} - 10^{11.5} M_{\odot}$ , with a weak dependence on redshift. They are also found to preferentially map different density environments at different stages of evolution of the Universe. At high redshifts, the observable host galaxies are predicted to be located in similar environments as the global galaxy population but to have a slightly higher probability to have a close companion.

**Key words:** gamma-rays: bursts – methods: numerical – stars: formation – galaxies: evolution, interactions.

## 1 INTRODUCTION

Gamma-ray bursts (GRBs) are brief pulses of  $\gamma$ -ray radiation observed on average once a day at random directions in the sky. They are the brightest sources in this region of the electromagnetic spectrum, and they have been systematically studied in the past two decades (e.g. Mészáros 2006, and references therein). The origin of GRBs is cosmological, as determined from the measurement of their redshifts

(e.g. Metzger et al. 1997; Bloom, Djorgovski & Kulkarni 2001; Bloom et al. 2003), and in many cases, their host galaxies have been identified (see Le Floch et al. 2003; Savaglio, Glazebrook & Le Borgne 2009, and references therein). Their distances imply the release of large amounts of energy ( $\sim 10^{51}$  ergs) in a short time-scale, which suggests that the origin of these phenomena could be associated to the accretion of matter onto a compact object (Woosley 1993; Fryer et al. 1999; MacFadyen & Woosley 1999; Panaitescu & Kumar 2001; Frail et al. 2001).

Two populations of GRBs are apparent from the distribution of their duration (Kouveliotou et al. 1993). Those lasting less than 2 s are known as short GRBs, while

\* E-mail: nchisari@princeton.edu (NECh); current address: Department of Astrophysical Sciences, Princeton University, Princeton, NJ 08544.

longer events are called long GRBs (LGRBs). These are more frequently observed and more precisely located, which makes their properties better known. LGRBs are always found in host galaxies with ongoing star formation activity (Le Floc'h et al. 2003; Christensen, Hjorth & Gorosabel 2004; Prochaska et al. 2004), and some of them were observed to be associated with Type Ib/c core-collapse supernovae (Galama et al. 1998; Hjorth et al. 2003). These observations suggest that the progenitors of LGRBs are massive stars. Stellar evolution models have tried to provide a consistent scenario where a LGRB can develop. The result is the so called *collapsar model* (Woosley 1993; Fryer, Woosley & Hartmann 1999), in which this phenomenon is produced during the collapse of a massive star, due to the accretion of part of the envelope onto the recently formed black hole. Nevertheless, the properties of LGRB progenitors (mass, metallicity, rotation velocity, binarity, etc.) are still a matter of discussion. LGRBs have been associated to single massive stars (Woosley 1993), perhaps in metallicity biased environments (Hirschi, Meynet & Maeder 2005), and also to stars in binary systems (Bissaldi et al. 2007).

The importance of understanding the nature of the LGRB progenitors is beyond the interest of only stellar evolution and black hole formation. Given their connection to massive stars and their large luminosities, LGRBs might be a powerful tool to investigate the star formation in the early Universe, at redshifts for which standard tools become ineffective (e.g. Wijers et al. 1998). The knowledge of the properties of the stellar progenitors would allow the assessment of possible biases originated when LGRBs are used as tracers of star formation. Several authors suggest that the cosmic LGRB rate does not follow the star formation rate (Daigne, Rossi & Mochkovitch 2006; Salvaterra & Chincarini 2007). The interpretation of their data requires the assumption of a differential evolution of the comoving LGRB rate density with respect to the co-moving star formation rate (SFR) density. The same conclusion arises from the work of Wolf & Podsiadlowski (2007), who show that the luminosity function of LGRB hosts differs from that of core-collapse supernovae hosts, which are considered unbiased tracers of star formation. According to these authors, the LGRB host luminosity function can be reproduced by requiring LGRB progenitors to have metal abundances lower than that of the Sun.

An indirect procedure to investigate LGRB progenitors is to characterise the stellar populations of their host galaxies. Given the connection between LGRBs and star formation, galaxy formation models can be used to assess the validity of LGRB progenitor models, comparing their predictions about the properties of these stellar populations to host galaxies observations. Recent works such as that of Kauffmann et al. (2004), suggest that there is a strong relation between star formation and nuclear activity in a galaxy with its environment, at constant stellar mass. Hence, the environment of host galaxies might constitute an independent probe for progenitor models. Observational works on host galaxies environment are still inconclusive on whether host galaxies inhabit regions with certain characteristics (Fynbo et al. 2002; Jakobsson et al. 2005; Thöne et al. 2008). Bornancini et al. (2004) suggest that host galaxies are field galaxies, while Wainwright, Berger & Penprase (2007)

find that a considerable fraction of their sample of 42 host galaxies shows evidence of interaction with other galaxies. The question of whether there is a connection between the occurrence of a LGRB and the local density of galaxies remains unanswered.

Since galaxy formation is a highly non-linear process, the properties of host galaxies predicted by different progenitor scenarios are better studied by means of cosmological numerical simulations (Katz & Gunn 1991; Navarro & White 1993; Mosconi et al. 2001; Springel & Hernquist 2003; Scannapieco et al. 2005, 2006). Courty, Bjornsson & Gudmundsson (2004) use hydrodynamical simulations of structure formation to identify a galaxy population whose properties reproduce the observed ones. According to these authors, the luminosity distribution of host galaxies is reproduced if galaxies are required to have high star formation efficiency. However, their simulations do not make any prediction on the properties of the LGRB progenitors. Nuza et al. (2007) developed a Monte Carlo code to simulate the production of LGRBs in hydrodynamical simulations of galaxy formation, assuming that their progenitors are massive stars as proposed by the collapsar model. These authors follow the LGRB production as the structure forms and evolves in the Universe. Their results suggest that LGRB progenitors would be low metallicity stars ( $Z < 0.3Z_{\odot}$ ), and hence LGRBs would be biased tracers of star formation principally at low redshift. However, their simulations explore a small volume of  $(10h^{-1} \text{ Mpc})^3$  dominated by field galaxies. Recently, Campisi et al. (2009) have constructed a simulated population of host galaxies based on the semi-analytic model of galaxy formation of De Lucia & Blaizot (2007) applied to cosmological simulations developed by Wang et al. (2008). These simulations describe a larger volume of the Universe (a square box of  $125h^{-1} \text{ Mpc}$  in a side). Campisi et al. (2009) explore three LGRB progenitor models based on the collapsar model, one of them assuming a given stellar mass value and an age cut-off and the other two also including metallicity cut-offs. These authors find that models with very low metallicity progenitors ( $Z < 0.1Z_{\odot}$ ) could explain the luminosities, colours and metallicities of the observed host galaxies. Their results support previous claims of LGRBs being biased tracers of the star formation.

Clearly, the use of larger simulations with better resolution and more detailed descriptions of the physical processes driving the dynamical, chemical and star formation histories of galaxies allows a better modelling of the host galaxies of LGRBs. However, an important aspect that should not be disregarded is that, for a proper comparison with observed host galaxies, the effects of the detectability of these galaxies must be taken into account. And this is the main contribution of our work where we developed an observational pipeline which allows us to mimic, at least in part, biases affecting the observations. With this new tool we build an observable host galaxy catalogue which can be more fairly compared to current available observations.

In this work, we develop a semi-analytical model for the host galaxies of LGRBs adopting the collapsar model for the progenitor stars. We apply it to one of the largest cosmological simulations available, the *Millennium Simulation* Springel et al. (2005). The *Millennium Simulation* follows the evolution of dark matter in a box of  $500h^{-1} \text{ Mpc}$  in a

side, hence providing a cosmologically representative volume a factor of 64 larger than that of Wang et al. (2008) and factor of  $\sim 10^5$  larger than that of Nuza et al. (2007). We take the galaxy catalogue built up by De Lucia & Blaizot (2007), who describe the evolution of baryonic matter including star formation, active galactic nuclei and supernova feedback. Using the star formation and chemical properties of galaxies in this catalogue to implement different LGRB progenitor scenarios, we determine the properties of the overall host galaxy population and its environment. We compute the detectability of the host galaxies in order to compare the predictions of these scenarios to the observations compiled by Savaglio et al. (2009).

This work is organized as following. In Section 2, we briefly describe the cosmological simulation and semi-analytic galaxy catalogue used in our work. In Section 3, we develop our implementation of LGRB progenitor scenarios. Sections 4 and 5 show our results on host galaxy properties and environment, respectively. Finally, Section 6 presents our conclusions.

## 2 MILLENNIUM SIMULATION

The *Millennium Simulation* (Springel et al. 2005) is one of the largest cosmological simulations of structure formation publicly available. It describes the evolution of the cold dark matter while the baryonic matter can be included via semi-analytic models on top of the numerical simulation. The *Millennium Simulation* describes the formation of structure tracking  $\sim 10^{10}$  dark matter particles of mass  $8.6 \times 10^8 h^{-1} M_\odot$  distributed in a cubic region of  $500 h^{-1} \text{Mpc}$  side, using the  $\Lambda$ CDM cosmogony. The adopted cosmological parameters are  $\Omega_m = 0.25$ ,  $\Omega_b = 0.045$ ,  $\Omega_\Lambda = 0.75$ ,  $\sigma_8 = 0.9$  and  $n = 1$ , where the Hubble constant is  $H_0 = 100 h \text{ km s}^{-1} \text{ Mpc}^{-1}$  with  $h = 0.73$ . These parameters are chosen in consistency with results obtained by the joint analysis of the Two-degree Field Galaxy Redshift Survey (2dFGRS<sup>1</sup>) and the Wilkinson Microwave Anisotropy Probe (WMAP) data (Sánchez et al. 2006).

The simulation was performed using a modified version of GADGET-2 hydrodynamical code (Springel 2005). A *friends-of-friends* (FOF) algorithm identified non-linear dark matter haloes within the simulation in an automatic manner. Two particles belong to the same halo if their separation is less than 0.2 times the mean separation between particles. Only groups of more than 20 particles are identified as haloes. This restriction sets a lower limit on the mass of a halo of  $1.72 \times 10^{10} h^{-1} M_\odot$ . Substructures orbiting within each virialized halo are identified applying a SUBFIND algorithm (Springel et al. 2001). Each dark matter halo has a central (Type 0) galaxy and one or more satellite galaxies. Satellites were at some point central galaxies of smaller haloes which suffered a merger with the halo they currently inhabit. There are two types of satellite galaxies, Type 1 galaxies are located at the centre of a subhalo associated with a FOF group, while Type 2 galaxies have lost their dark matter subhalo after falling onto a more massive halo.

Mean properties of synthetic galaxies (e.g. SFR, stellar mass, gas mass, metallicity) are obtained by applying semi-analytic models to the structure formation simulation (White & Frenk 1991; Cole 1991; Lacey & Silk 1991). Essentially, semi-analytical models describe the collapse of baryonic matter following dark matter haloes. After collapsing, the gas cools and gravitational instabilities produce episodes of star formation. To reproduce observations, models incorporate photoionization processes in the intergalactic medium, the growth of supermassive black holes during galactic mergers, supernova and AGN feedback, star formation rate enhancement in mergers, and formation of heavy elements for each formed stellar population. The galaxy catalogue we use in this work is that of De Lucia & Blaizot (2007).

There is recent evidence for an excessive reddening of Type 2 galaxies (Weinmann et al. 2006; Perez, Tissera & Blaizot 2009) which might be due to the poor physical treatment of this type of galaxies. In order to avoid spurious trends, we exclude Type 2 galaxies from our analysis in Section 3 and Section 4. However, Type 2 galaxies ought to be included in the environmental analysis performed in Section 5 in order to correctly trace the underlying mass distribution.

Hence, the catalogue of De Lucia & Blaizot (2007) provides us with the spatial galaxy distribution, their stellar masses, dark matter haloes, star formation activity, colours, luminosities and mean metallicities. Regarding the latter, the public catalogue makes available the mean metallicity of the cold gas component and of the stellar population as a whole (i.e. averaged over new and old stars in a galaxy). Therefore, as a proxy for the metallicity of the LGRB progenitors, we take the mean metallicity of the cold gas component at the time these stars were born. Because the De Lucia & Blaizot (2007) model assumes instantaneous recycling, this metallicity is slightly higher than that of the newly born stars, but this correction is negligible compared to the uncertainties in the measured metallicities (e.g. Campisi et al. 2009).

## 3 SCENARIOS FOR LGRB PROGENITORS

### 3.1 Intrinsic LGRB rate

We consider two scenarios for LGRB production, both of them based on the collapsar model (Woosley 1993; MacFadyen & Woosley 1999; Fryer et al. 1999). In our scenario I we take as LGRB progenitors all stars above a certain minimum mass  $m_{\min}$ , with no other restriction whatsoever. In this scenario LGRBs are unbiased tracers of star formation. Accordingly, we obtain the intrinsic LGRB rate in a given galaxy  $g$  at a particular redshift  $z$  as

$$r_{\text{GRB}}(g, z) = \text{SFR}(g, z) \frac{\int_{m_{\min}}^{100 M_\odot} \xi(m) dm}{\int_{0.1 M_\odot}^{100 M_\odot} m \xi(m) dm}, \quad (1)$$

where  $0.1 M_\odot$  and  $100 M_\odot$  are the lower and upper mass cut-offs of the IMF  $\xi(m)$  given by Chabrier (2003). According to Eqn. 1, the production of LGRBs is not delayed with respect to the starburst that created the progenitor stars, which is justified because in the collapsar model only massive stars are LGRB progenitors.

<sup>1</sup> <http://www.mso.anu.edu.au/2dFGRS/>

In our scenario II, we assume that only massive stars ( $m > m_{\min}$ ) below some metallicity threshold ( $Z_C$ ) are able to produce LGRBs, as in the progenitor models of Hirschi et al. (2005) or Yoon, Langer & Norman (2006). As explained before, we take the mean metallicity of cold gas in each galaxy as representative of the metallicity of the progenitor stars. The consequences of this hypothesis will be discussed in later sections. In this scenario, the intrinsic LGRB rate is given by Eqn. 1 for galaxies  $g$  with metallicity  $Z_g < Z_C$ , and is null for those with  $Z_g \geq Z_C$ . Three realizations of this scenario were computed, adopting  $Z_C = 0.1, 0.3, 0.6 Z_\odot$  (scenarios II.1, II.2 and II.3, respectively).

### 3.2 Observed LGRB rate

Given a metallicity threshold, we adjusted the only free parameter of our scenarios ( $m_{\min}$ ) to reproduce the LGRB rate measured by the BATSE experiment. For this purpose, we took the off-line GRB search of Stern et al. (2001), which detected 3475 GRBs with  $T_{90} > 2$  s during a live-time of 6.37 yr (70 per cent of the 9.1 yr that BATSE was active), scanning 67 per cent of the sky. This translates into a full-sky LGRB rate of  $814 \text{ yr}^{-1}$  above the threshold of the off-line search. The choice of this particular experiment was motivated by its good statistics and the availability of an accurate model for its detection efficiency.

To obtain the observable rate predicted by a given scenario, we first compute the comoving LGRB rate density for each redshift as

$$n_{\text{GRB}}(z) = V^{-1} \sum_g r_{\text{GRB}}(g, z), \quad (2)$$

where  $V = (500 h^{-1} \text{ Mpc})^3$  is the comoving volume of the *Millennium Simulation*. The full-sky observed LGRB rate is then

$$R_{\text{GRB}} = \int_0^{z_{\max}} \frac{n_{\text{GRB}}(z)}{(1+z)} p_{\text{det}, \text{BATSE}}(z) \frac{dV}{dz}, \quad (3)$$

where

$$\frac{dV}{dz} = \frac{4\pi c d_L^2(z)}{H(z)(1+z)^2} \quad (4)$$

is the derivative of the comoving volume with respect to  $z$  at fixed solid angle,  $z_{\max}$  is the maximum redshift of the simulation,  $d_L$  the luminosity distance and  $H$  the Hubble constant at redshift  $z$ , and  $p_{\text{det}, \text{BATSE}}$  the probability of detecting a LGRB at redshift  $z$  with BATSE (i.e. the probability that a particular LGRB has a peak flux above the experiment threshold). The integration was performed numerically, and the described procedure iterated over  $m_{\min}$ , until agreement with the observed rate was attained.

The value of  $p_{\text{det}, \text{BATSE}}(z)$  depends on the LGRB luminosity function and spectrum. It was computed using a Monte-Carlo scheme to simulate, at a given redshift, a large population of LGRBs with different luminosities and spectra. Then, their photon fluxes in the BATSE energy band were estimated. For each LGRB in this population, a second Monte-Carlo procedure rejected those events which would be undetectable, taking into account the trigger efficiency of the Stern et al. (2001) off-line search. If the LGRB emission were isotropic, the fraction of retained LGRBs would di-

**Table 1.** Main characteristics of our scenarios for the simulated host galaxies of LGRBs. Column (1) gives the name of the scenario. Column (2) lists the minimum stellar mass obtained for progenitor stars of LGRBs to reproduce BATSE observations, adopting Chabrier (2003) IMF. Column (3) gives the cold gas maximum metallicity cut-off. Column (4) shows ratio between the percentage of simulated host galaxies over the mass range  $\approx 10^{8.5-10.3} M_\odot$  and the corresponding value obtained from the sample of Savaglio et al. (2009).

Scenarios	$m_{\min} (\text{M}_\odot)$	$Z_C$	$R_M$
I	$91.4 \pm 0.1$	-	0.82
I.1	$13.9 \pm 0.2$	0.1	0.02
II.2	$44.3 \pm 0.4$	0.3	0.51
II.3	$76.0 \pm 0.3$	0.6	1.03

rectly give the detection probability due to the off-line search threshold. To account for the beamed emission of LGRBs (e.g. Yonetoku et al. 2005), and assuming that the distribution of jet opening angles is independent of the LGRB luminosity, spectrum and redshift, we obtain  $p_{\text{det}, \text{BATSE}}$  by multiplying this fraction by the mean beaming fraction of the jets  $p_{\text{jet}} = 10^{-3}$ . The luminosity function and spectral parameters distributions were taken from Daigne et al. (2006).

This procedure not only allows us to mimic the observational process but also has provided us with estimates of the minimum mass for the progenitor stars. The values of  $m_{\min}$  obtained, in solar masses, are  $91.4 \pm 0.1$ ,  $13.9 \pm 0.2$ ,  $44.3 \pm 0.4$ , and  $76.0 \pm 0.3$  for scenarios I, II.1, II.2 and II.3, respectively; the uncertainties reflect Poissonian errors in the number of observed LGRBs (see also Table 1).

### 3.3 Host galaxies

A meaningful definition of a LGRB host galaxy in our scenarios is not as straightforward as it might seem at first sight. The naïve definition of a host galaxy, at a given redshift  $z$ , as being any galaxy  $g$  with a LGRB rate of  $r_{\text{GRB}}(g, z) > 0$  (or identically,  $\text{SFR}(g, z) > 0$ ) is not useful because the resulting host population would include galaxies with arbitrarily low LGRB rates. Low rates are better understood in statistical terms, as very low probabilities of producing a LGRB per unit time. This implies that the corresponding galaxies have a low probability of being observed as host galaxies. Hence, this naïve definition would generate a host galaxies sample biased to low SFR galaxies. To fix this problem, the definition of a host galaxy could be based on the number of LGRBs  $N(g, z) = r_{\text{GRB}}(g, z)\Delta t$  produced in each galaxy during a time interval  $\Delta t$  in its rest frame, so that host galaxies are only those with  $N(g, z) \geq 1$ , as in Campisi et al. (2009). However this cut-off, and the resulting population, would be dependent on the more or less arbitrary choice of  $\Delta t$ .

Given the above arguments, we preferred instead a probabilistic approach, defining the likelihood of a galaxy being observed as a LGRB host. This likelihood is then used as a weight to compute the properties of the observable host galaxies sample, which would be in this way comparable to the observed sample. For a galaxy to be detected as a host at least one LGRB must be detected within it by a high-energy

observatory. Then, the galaxy itself must be detected, usually by optical/NIR telescopes. We would treat the biases introduced by each of these observations separately.

To model the first bias, we compute the probability of detecting at least one LGRB within it by any of the high-energy observatories monitoring GRBs. Given that event detection processes follow Poissonian statistics, if  $R_{\text{GRB},i}(g, z)$  is the contribution of galaxy  $g$  at redshift  $z$  to the LGRB rate observed by experiment  $i$ , the probability of observing at least one LGRB in a galaxy is

$$p_{\text{HG}}(g, z) = 1 - \exp \left( - \sum_i R_{\text{GRB},i} \Delta T_i \right), \quad (5)$$

where  $\Delta T_i$  is the time interval of the LGRB search conducted by experiment  $i$ . Eqn. 5 assumes that the searches by different observatories are independent. Previous works estimate the intrinsic LGRB rate in a typical galaxy to be of the order of  $10^{-3} \text{ yr}^{-1}$  (Fryer et al. 1999), hence the LGRB rate observed in the galaxy by any mission must be lower than this value. Given that current searches for LGRBs have spanned a few years,  $\sum_i R_{\text{GRB},i} \Delta T_i \ll 1$ , and  $p_{\text{HG}}(g, z) \simeq \sum_i R_{\text{GRB},i} \Delta T_i$ , which means that the likelihood of a galaxy being observed as a host is proportional to its contribution to the mean *observed* number of LGRBs,

$$p_{\text{HG}}(g, z) \simeq \frac{r_{\text{GRB}}(g, z)}{V(1+z)} \frac{dV}{dz} \sum_i p_{\text{det},i}(z) \Delta T_i \frac{\Delta \Omega_i}{4\pi}, \quad (6)$$

where  $\Delta \Omega_i$  is the sky coverage of the experiment  $i$ . Note that, for a fixed  $z$ , cosmological and observatory dependent factors in Eqn. 6 become constant, independently of the number of observatories considered, and cancel out in the normalization of the weights. This means that when computing mean HG properties such as mass or SFR as a function of  $z$ , the first bias can be modeled simply by weighting the corresponding properties of each galaxy by its *intrinsic* LGRB rate.

In the computation of the integrated properties of the whole population of host galaxies (like the integrated mass distribution, for example), also the effects of volume variation, time dilation and detectability of the different observatories must be taken into account (Pellizza et al. in preparation). In this case it is better to compute first the mass distribution observed by each experiment at each redshift  $z$ , weighting the galaxies in the corresponding snapshot by  $p_{\text{HG}}(g, z)$ . Second, the integration in  $z$  can be performed for each experiment, and the resulting distribution can be normalized. This has the advantage of avoiding the use of the values of  $\Delta T_i$  and  $\Delta \Omega_i$ , which are poorly known for some of the observatories that detected the LGRBs in the sample of Savaglio et al. (2009). Only  $p_{\text{det},i}(z)$  for each experiment is needed, which is computed as described in Sect. 3.2 for  $p_{\text{det},\text{BATSE}}(z)$ . Finally, these distributions can be combined into a single one by adding them, previously scaled to the number of LGRBs detected by each observatory. The relevant data for computing the detectability were taken from Stern et al. (2001) for BATSE, Guetta & Piran (2007) for *Swift*, Frontera et al. (2009) for *Beppo-SAX*, Pélangeon et al. (2008) for *HETE-2* and Hurley et al. (1992) for *Ulysses*. These experiments detected 36 of the 38 LGRBs in the sample of Savaglio et al. (2009). For statistical reasons, only experiments that detected at least five LGRBs in

the sample were considered. Konus-*Wind* and *NEAR-XGRS* were discarded because all their LGRBs were observed also by other experiments above. To be consistent, the observed mass distribution to which the model predictions were compared was constructed from the data of Savaglio et al. (2009) by adding the individual distributions observed by each experiment.

The second bias is more difficult to model. Given that the search for host galaxies is guided by the discovery of the LGRBs themselves and usually done with a variety of different telescopes and detectors, in different bands of the electromagnetic spectrum and with different sensitivities, the biases introduced are unclear. Galaxies with surface brightness below the detectability threshold of available instruments could introduce a bias towards low metallicity galaxies. An extra problem could be caused by dust obscuration which could affect the detection of the afterglows and produce a bias towards high metallicity galaxies (Fynbo et al. 2009). Hence, at least these two effects might combine themselves to determine the detectability of a host galaxy. Considering also the fact that we have only access to the public galaxy catalogue of the *Millennium Simulation* which provides only mean global properties and magnitudes, we adopt the observed integrated stellar mass distribution as a tool to apply the combined effect of observational biases to the simulated galaxy sample. We use the fact that the observed integrated stellar mass distribution has been affected by observational biases although we cannot disentangle their individual effects. Hence, we require the simulated LGRB hosts to reproduce the observed stellar mass distribution in order to build up the observable simulated LGRB hosts. The procedure is explained in detail in next section. Note that, hereafterin, we will discuss the trends of the observable simulated hosts and the general galaxy population. The former can be compared to the current observed hosts, but, if this later sample changes due to better or different observational techniques, our simulated sample should be also consistently modified to match the new observed stellar mass distribution.

#### 4 LGRB HOST PROPERTIES

The largest and most comprehensively uniform sample of host galaxy properties available at present is that compiled by Savaglio et al. (2009)<sup>2</sup>. Stellar masses, star formation rates, metallicities, absolute magnitudes and colours of 46 observed host galaxies up to  $z \sim 3$  were obtained by these authors comparing their spectral energy distributions to those of synthetic stellar populations, using the method described in Glazebrook et al. (2004).

A key point of our models is that we require the stellar mass distribution of the predicted host galaxies to match that of the observed host galaxies. The stellar mass is adopted as the property to be reproduced by the models since it is now widely accepted that stellar mass is a more fundamental quantity for galaxies than luminosity (e.g. Kauffmann et al. 2004). It could be possible that those LGRB events with no detected hosts occurred in very low surface brightness galaxies and hence, with low stellar masses.

<sup>2</sup> Data available at <http://www.grbhosts.info>

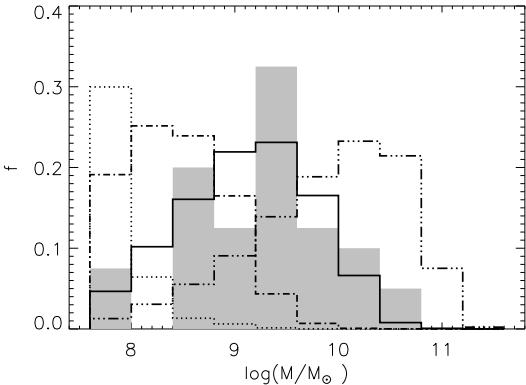


**Figure 1.** Stellar mass distribution of host galaxies in the sample of Savaglio et al. (2009) (shaded in gray), together with those predicted by scenarios I (dashed-triple dotted line), II.1 (dotted line), II.2 (dashed-dotted line) and II.3 (solid line).

As mentioned before the effects of dust could also prevent the detection of events in high metallicity (and dusty) galaxies. In our models these host galaxies exist (and are part of the global galaxy population) but the observability cut-off has been determined by using the current observed stellar mass distribution. Fig. 1 shows the distribution of stellar masses of observed host galaxies constructed from the data of Savaglio et al. (2009), together with those predicted by our scenarios.

As it can be seen from Fig. 1, the scenario which best reproduces the observed stellar mass distribution is that with  $Z_C = 0.6 Z_\odot$  (scenario II.3, see also Table 1). Lower metallicity thresholds predict lower observed stellar masses for the host galaxies, while no metallicity threshold (scenario I) predicts larger ones. In the sample of Savaglio et al. (2009), we find that 85 per cent of the studied galaxies have stellar masses over the range  $\approx 10^{8.5-10.3} M_\odot$  (see also Castro Cerón et al. 2008). The probability of getting a host galaxy within this stellar mass range in scenario II.3 is 88 per cent, while for scenarios I, II.1 and II.2 it is 70, 2, and 43 per cent, respectively. Then we conclude that scenario II.3 predictions agree fairly well with observations while others fail, and therefore in the following sections, we will focus only on this scenario.

We stress the fact that its predictions include the effects of host galaxies observability, hence, a proper comparison with observations can be made. In order to contribute to the understanding of the nature of LGRB host galaxies, we will also compare these predictions with the properties (not weighted by host galaxy observability) of both the sample of all galaxies with mean cold gas metallicities below  $0.6 Z_\odot$  (hereafter low metallicity sample) and the complete galaxy population of the catalogue of De Lucia & Blaizot (2007).

#### 4.1 Stellar mass

As a first step towards understanding the nature of host galaxies, we analyse their stellar masses as a function of redshift. As shown in Fig. 2, the mean stellar mass of the host galaxies as a function of redshift predicted by scenario II.3 reproduces the observed mean trend quite well. From this

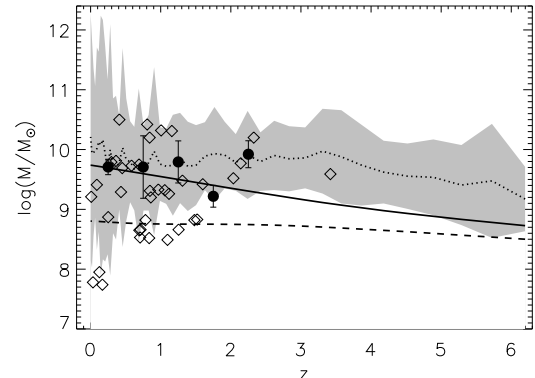


**Figure 2.** Mean stellar mass of the host galaxies as a function of redshift predicted by scenario II.3 (dotted line) with its standard deviation (shaded grey band). Open diamonds represent the observed host galaxies of Savaglio et al. (2009), while filled circles correspond to their mean values in redshift intervals of 0.5. For comparison, we also include the corresponding mean trends for the low metallicity sample (dashed line) and the complete galaxy population (solid line).

figure, we can also see that host galaxies are, on average, more massive than galaxies in the complete galaxy population while the latter are more massive than those in the low metallicity sample. This can be understood taking into account that the host galaxy observability is a strong function of the star formation rate, and that the complete galaxy population in the catalogue of De Lucia & Blaizot (2007) follows a mass-metallicity relationship (e.g. De Rossi et al. 2009). Then, the cut-off adopted for the mean cold gas metallicity to reproduce the observed stellar mass distribution implies a cut-off in stellar mass since low metallicity galaxies are, on average, less massive than the general galaxy population (see also Fig. 1). However, as the observability of a host galaxy depends strongly on its star formation activity and most of the small galaxies have low star formation rates, the observable host galaxies tend to be, on average, the more massive ones among them. As a result, our observable sample tends to be populated by systems more massive than those in the low metallicity sample or in the complete galaxy population.

#### 4.2 Star formation rate

In Fig. 3, we display the mean SFR of host galaxies as a function of redshift predicted by scenario II.3, together with the corresponding mean values for the low metallicity sample and the complete galaxy population. As it can be seen, the prediction of scenario II.3 reproduces very well the behaviour of the observed host galaxies. These have higher SFR than the mean of the complete galaxy population, and much higher than that of the low metallicity sample. The good agreement between our scenario II.3 and observations suggests that the observed host galaxies are biased towards galaxies with stellar masses in the range  $10^{9-10} M_\odot$ , high star formation activity and relatively low gas metal content, compared to the mean properties of the complete galaxy population at a given  $z$ .

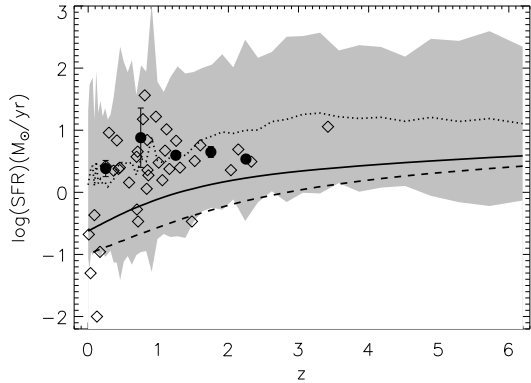


**Figure 3.** Mean SFR of the host galaxies as a function of redshift predicted by scenario II.3 (dotted line) with its standard deviation (shaded grey band). Open diamonds represent the observed host galaxies of Savaglio et al. (2009), while filled circles correspond to their mean values in redshift intervals of 0.5. For comparison, we also include the corresponding mean trends for the low metallicity sample (dashed line) and the complete galaxy population (solid line).

Regarding the mean specific SFR (SSFR), defined as the ratio between the SFR and the stellar mass of a given galaxy (Fig. 4), host galaxies are predicted to show SSFRs similar to those in the low metallicity sample, and higher than those in the complete galaxy population, for  $z < 2$ . Between  $z \sim 2$  and  $z \sim 6$ , there are no significant differences in mean SSFRs among the three samples, which have larger SSFRs than low redshift galaxies. This can be understood because, at higher redshift, galaxies have larger gas reservoirs which can feed stronger star formation activity and are, on average, less chemically enriched. At low redshift, host galaxies seem to be particularly efficient at transforming gas into stars. Note, however, that the mean SSFR predicted by scenario II.3 at low redshift is half an order of magnitude lower than the mean observed SSFR.

#### 4.3 Luminosity and colour

Observations show that host galaxies tend to be bluer than the general population of galaxies observed at a given redshift, and fainter than a typical  $L^*$  galaxy. In fact, this trend can be nicely reproduced by our scenario II.3, as shown in Fig. 5. The luminosities and colours of the predicted host galaxies are in excellent agreement with the observations compiled by Savaglio et al. (2009). From this figure, we can see that host galaxies are bluer than the complete galaxy population for  $z < 2$ , but have similar mean colours for higher redshifts. Our scenario predicts that host galaxies are more luminous systems in the  $B$ -band, compared to the mean luminosity of the global galaxy population at all redshifts.

#### 4.4 Metallicity

In Fig. 6, we compare the mean cold gas metallicity of the host galaxies predicted by scenario II.3 to different metallicity estimations reported by Savaglio et al. (2009). Since

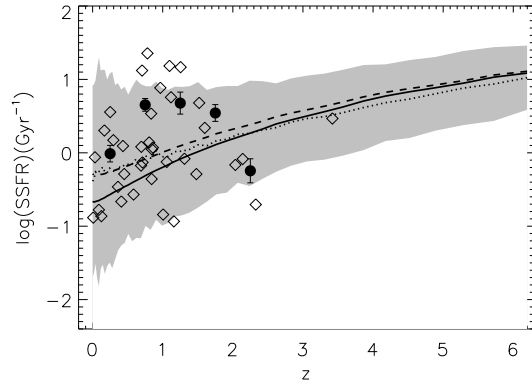


**Figure 4.** Mean SSFR of the host galaxies as a function of redshift predicted by scenario II.3 (dotted line) with its standard deviation (shaded grey band). Open diamonds represent the observed host galaxies of Savaglio et al. (2009), while filled circles correspond to their mean values in redshift intervals of 0.5. For comparison, we also include the corresponding mean trends for the low metallicity sample (dashed line) and the complete galaxy population (solid line).

at  $z > 0.2$  it is very difficult to distinguish HII regions with enough resolution, these authors generally measured the optical luminosity-weighted mean metallicity in a galaxy. For consistency, host galaxies at  $z < 0.2$  were treated by them as the rest of the sample (i.e. integrating fluxes over the whole galaxy). In this figure, we have included metallicities obtained by using different indicators (see Savaglio et al. 2009, for more details). In some cases, absorption lines in the optical afterglow can be used to obtain the metallicity of neutral cold gas along the line of sight of the GRB (the so-called GRB-DLAs). This is the case of 9 GRB-DLA systems studied by Savaglio (2006), all of them at  $z > 1.6$ . In this case, the metallicity could be associated more directly to the metallicity of the host galaxy, contrary to QSO-DLAs which are associated to HI clouds in the intergalactic medium. At  $z < 1$ , measurements of metallicity by Savaglio et al. (2009) are derived from hot gas and, in this case, the lower branch solution is preferred for the hosts. As shown in Fig. 6, the predicted host galaxies metallicities are systematically higher than the GRB-DLA metallicities. This might indicate that LGRBs occur in regions of even lower metallicity than the mean metallicity of the cold gas of the host galaxies. In this sense, Nuza et al. (2007), adopting similar hypotheses to generate synthetic LGRB populations, but using full cosmological simulations where the chemical enrichment of baryons was consistently followed with redshift, claimed a metallicity threshold of  $0.3Z_\odot$  for the progenitor stars in order to reproduce observations. More detailed information on the metallicity of individual stellar populations, which also takes into account the inhomogeneities of the interstellar medium, are needed to improve our understanding of this issue (see Pontzen et al. 2009 and Artale et al. in preparation). Also along these lines, a work by Modjaz et al. (2008) compares the metallicity of GRB hosts associated to Type Ic supernovae (SN Ic) to broad-line SN Ic without GRB detection at  $z < 0.25$ . The metallicity of SN-GRB host galaxies are estimated by computing the nebular oxygen abundance

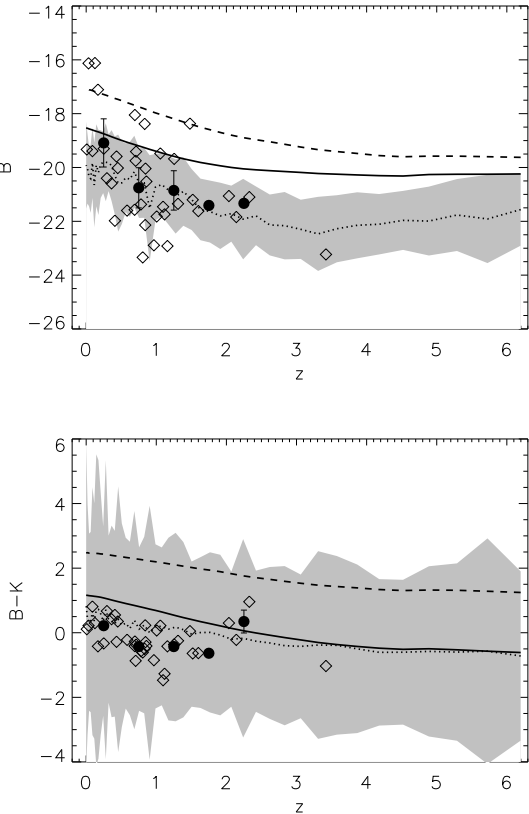


**Figure 5.** Mean  $B$ -band luminosity (upper panel) and  $B - K$  colour (lower panel) as a function of redshift predicted by scenario II.3 (dotted line) with its standard deviation (shaded grey band). Open diamonds represent the observed host galaxies by Savaglio et al. (2009), while filled circles correspond to their mean values in redshift intervals of 0.5. For comparison, we also include the corresponding mean trends for the low metallicity sample (dashed line) and the complete galaxy population (solid line).

by three different methods. In this case, they directly probe the environments of the progenitors because either they were measured at that location or they correspond to metallicities of homogeneous dwarf galaxies. Modjaz et al. (2008) results are in agreement with the values obtained by Savaglio et al. (2009) and with our own results at low redshifts.

## 5 ENVIRONMENT OF LGRB HOSTS

It is still under discussion if host galaxies are always located in regions of a given characteristic local density or if, depending on  $z$ , they inhabit different environments. Recently, Campisi et al. (2009) estimated the cross-correlation function of their simulated host galaxies finding that these systems tend to map underdense regions. Observations provide somehow contradictory results. Bornancini et al. (2004) found host galaxies to inhabit field regions. Lately, Wainwright et al. (2007) suggested that host galaxies might be biased towards interacting or merging galaxies. It is yet too soon for observations to provide a robust answer to these questions but theoretical predictions could positively contribute to this area. The advantage of our model is that

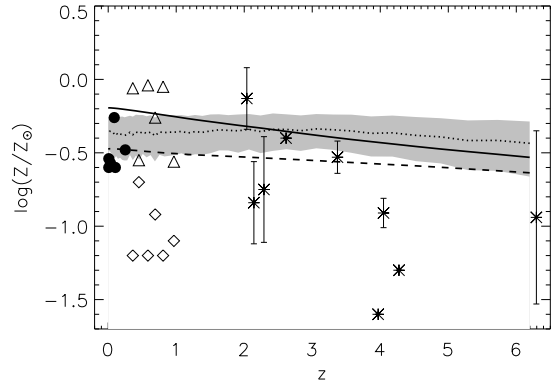


**Figure 6.** Mean cold gas metallicity as a function of redshift predicted by scenario II.3 (dotted line) with its standard deviation (shaded grey band). Filled circles represent observed metallicities of host galaxies reported by Savaglio et al. (2009), measured using the  $T_e$  technique. We also include those measured by the R32 upper branch (triangles) or lower branch (diamonds), and GRB-DLAs (asterisks). For comparison, we include the corresponding mean trends for the low metallicity sample (dashed line) and the complete galaxy population (solid line).

taking into account the observability allows us to make a more robust prediction.

In this section, we investigate the environment of the simulated host galaxies by means of three different estimators. The distance to the closest neighbour ( $d_1$ ) of a host galaxy provides an estimation of the possibility of a host galaxy being interacting with another galaxy. The distance to the fifth neighbour ( $d_5$ ) of a host galaxy provides an estimation of the density of the region the galaxy inhabits. Finally, the central halo virial mass ( $M_{\text{vir}}$ ) is an estimator of the global potential well to which the host galaxy is bound.

In the particular case of the closest neighbour, it is well known that pair interactions can enhance the star formation activity (e.g. Lambas et al. 2003; Patton et al. 2005) and if LGRB progenitors are massive stars this would imply an increase in the probability of detecting a LGRB event. Since semi-analytical codes do not model tidally-induced star formation, we modified the SFR for galaxies with their closest neighbour located at distances smaller than  $0.1h^{-1}$  Mpc by a factor of two, motivated by observational and numerical results (e.g. Lambas et al. 2003; Perez et al. 2006, 2009; Di Matteo et al. 2008). However, this correction does not change any of the trends reported in this work. But the role of interactions should be further tested with models that properly include their effects.

We estimate the cumulative distribution of these three environmental estimators ( $d_1, d_5, M_{\text{vir}}$ ) predicted by scenario II.3. To quantify behaviours as a function of redshift, we determine the values  $d_{1,50}, d_{5,50}$  and  $M_{\text{vir},80}$  at which the corresponding cumulative fractions reach 50 per cent in the case of  $d_1$  and  $d_5$ , and 80 per cent in the case of  $M_{\text{vir}}$ . In Fig. 7 (upper panel), we show  $d_{1,50}$  as a function of redshift according to scenario II.3, together with the trend for the low-metallicity sample and the complete galaxy population. At high redshift, the three samples tend to have the nearest neighbour at approximately similar distances. We only

note a slight trend for host galaxies to systematically have a closer first neighbour than galaxies in the other two samples for  $z > 1$ . From  $z \sim 1$ , low metallicity galaxies tend to have their closest neighbour further away than either a galaxy in the complete population or a host galaxy. The latter tend to inhabit lower density regions than galaxies in the complete population. Our models indicate that observable host galaxies would only have a slightly higher probability to be in a galaxy pair compared with the general galaxy population at high redshift (i.e. 50 per cent of galaxies have the first neighbour closer than  $\sim 50$  kpc).

The global environment is quantified by  $d_{5,50}$ . As shown in Fig. 7 (middle panel) at high redshift ( $z > 2$ ), galaxies in the three samples reside in similar environments. For lower redshift there is a clear trend for galaxies in the low metallicity sample and host galaxies to inhabit lower density regions than galaxies in the complete galaxy population. This results agree with the numerical work of Campisi et al. (2009), and also with the observational findings of Bornancini et al. (2004), taking into account that the mean redshift of LGRBs observed at that time was  $\langle z \rangle < 2$ .

In the case of the virial mass, as shown in Fig. 7 (lower panel), we find that 80 per cent of observable host galaxies have haloes less massive than  $10^{11.0-11.5} M_\odot$  at any redshift. As the structure forms and groups and clusters aggregate hierarchically, galaxies tend to inhabit larger dark matter haloes. However, host galaxies stay within a narrower range of mass haloes. The inversion in the relation observed in this figure can be understood considering that host galaxies observability depends strongly on the star formation activity which, in turn, depends strongly on environment (Poggianti et al. 2009). Hence, from  $z \sim 2$  active star forming galaxies (i.e. those which are important generators of LGRBs) with mean stellar masses of  $\sim 10^{10} M_\odot$  reside again in slightly smaller dark matter haloes (Fig. 2 and Fig. 3). Note that this is not the case for the general low metallicity sample which although residing, on average, in smaller haloes than the global galaxy population, tend to systematically inhabit larger ones with decreasing redshift, as expected in a hierarchical scenario. The observability condition which is closely linked to the star formation activity produces this kind of halo downsizing scenario for host galaxies at low redshift, while the mean stellar mass remains approximately constant.

## 6 CONCLUSIONS

Our results indicate that the observed LGRB host galaxies properties can be reproduced assuming that LGRB progenitors are massive stars and occur in galaxies with moderately low mean cold gas metallicities. The joint requirement for the synthetic LGRBs to reproduce the observations of BATSE and for the simulated systems that host them to reproduce the stellar mass distribution of the observed host galaxies determines the minimum mass for the progenitor star ( $m > 75 M_\odot$ )<sup>3</sup> and the maximum metallicity cut-off

<sup>3</sup> The mass threshold for LGRB progenitors was computed for the Chabrier (2003) IMF used in the catalogue of De Lucia & Blaizot (2007), and would be  $54 M_\odot$  if a Salpeter (1955) IMF had been used, instead.

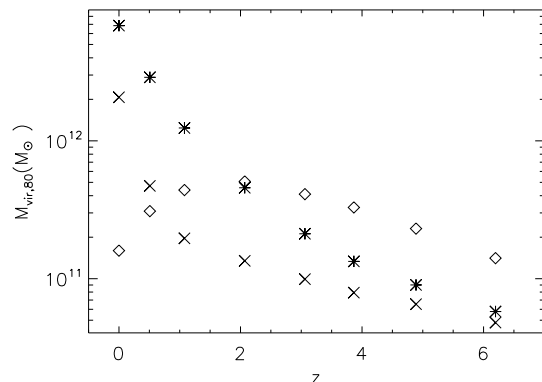
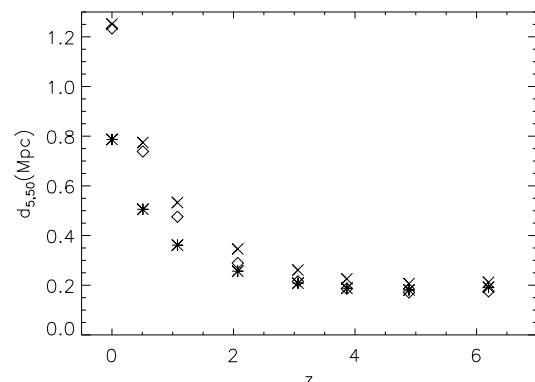
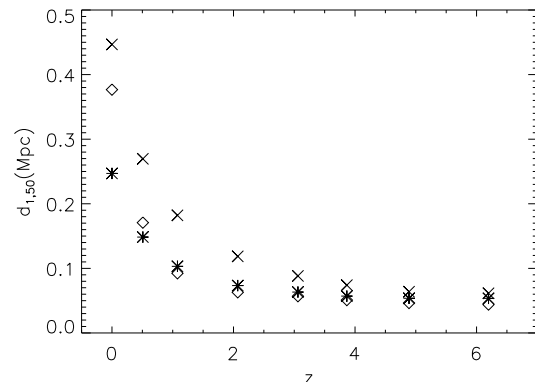


**Figure 7.** Environmental study of host galaxies predicted by scenario II.3 (diamonds), the complete galaxy population (stars), and the low metallicity galaxy sample (crosses). *Upper panel:* Median distance to the closest neighbour ( $d_{1,50}$ ). *Middle panel:* Median distance to the fifth neighbour ( $d_{5,50}$ ). *Left panel:* Virial mass of the central halo at the 80 percentile ( $M_{\text{vir},80}$ ).

( $0.6 Z_\odot$ ) for the cold gas metallicity of the simulated host galaxies. Our scenario II.3, which satisfies these conditions, succeeds at reproducing the dependence on redshift of stellar mass, luminosity, colour, SFR, SSFR and metallicity of the observed host galaxies compiled by Savaglio et al. (2009) over the redshift range  $0 < z < 3$ .

Our main findings are:

- (i) The average stellar mass of host galaxies is higher than the average stellar mass of the complete galaxy population,

and remains within a narrow mass range around  $10^{10} M_{\odot}$ , with a very weak trend to lower mass for higher redshifts, due to the double requirement of low mean gas metallicity and high star formation rates. We note that the dispersion is approximately 0.5 dex around the log mean stellar mass.

(ii) Compared to the characteristic stellar mass  $M^* \sim 10^{10.63} M_{\odot}$  estimated by Bell et al. (2003), host galaxies are low stellar mass systems (88 per cent of our host galaxies have stellar masses between  $\sim 10^{8.5-10.3} M_{\odot}$ ). However, compared to the mean stellar mass of the complete galaxy population, host galaxies tend to be massive galaxies.

(iii) The SFR of host galaxies is larger than that of galaxies in the complete population at all redshifts. At  $z > 2$ , the SSFR of observable host galaxies is comparable to the complete galaxy population, but at lower redshift it is systematically higher. As a consequence, host galaxies are, on average, bluer than the global galaxy population. The dispersion found for the properties of the observable host galaxies reflect the different histories of formation of galaxies at a given stellar mass.

(iv) Our results support the claims for a metallicity threshold to reproduce the properties of the current observed host galaxies. The global metallicity threshold of  $0.6 Z_{\odot}$  we derived from our models is an upper limit for the metallicity of the LGRB progenitor stars in the case of no dust effects. The comparison of the mean metallicity of host galaxies predicted by our model with GRB-DLAs observations suggests that LGRBs might be produced in stars of even lower metallicity as pointed out by other authors (e.g. Nuza et al. 2007; Campisi et al. 2009). At low redshift, our results are in agreement with SN-GRB local metallicity estimations by Modjaz et al. (2008). However, observations show a large spread in metallicity and there are also observational uncertainties that can affect its determination. Hence, results should be taken with caution.

(v) For  $1 < z < 6$ , host galaxies seem to be slightly more likely to be in pairs than galaxies belonging to the other samples. There is, however, a change of behaviour for  $z < 1$ , where the at least 50 per cent of the host galaxies seems to have their closest neighbour further away than galaxies in the complete population, but closer than galaxies in the low metallicity sample. We highlight that we are considering neighbouring galaxies of a mass above  $10^9 M_{\odot}$ . This limit is set by the numerical resolution of the *Millennium Simulation*. Lower mass companions could also imprint morphological perturbations and trigger star formation activity (e.g. Lambas et al. 2003) but we cannot pursue this analysis further on with this galaxy catalogue.

(vi) Regarding global environment, our model suggests that, at  $z > 1$ , observable host galaxies would preferentially inhabit environments of similar density to those populated by the general population and of slightly higher density than those inhabited by the low metallicity sample. Towards  $z = 0$ , observable host galaxies tend to be progressively located in less dense environments, which becomes as subdense as the regions where low metallicity galaxies reside (see also Campisi et al. 2009).

(vii) Our results suggest that observable host galaxies tend to have dark matter haloes in the range  $10^{11.0-11.5} M_{\odot}$ , regardless of redshift, and show a slight signal for halo down-sizing from  $z \sim 1$ , distinguishing them from the other two samples which follow the expected halo mass growth in a hi-

erarchical scenario. This result is consistent with observable host galaxies being systems with mean stellar masses approximately constant, regardless of the age of the Universe.

Our results are mainly a consequence of the joint requirements to have high star formation activity to ensure observability and to reproduce the current distribution of stellar masses of observed host galaxies. However, within the current constraints, galaxies with high masses would be too metal-rich to produce LGRBs and low mass systems would have low probability of being observed. If the observed sample were modified by the incorporation of other galaxies, for example dusty hosts, then our model would need to be readjusted accordingly.

## ACKNOWLEDGMENTS

We thank M.E. De Rossi and Gerard Lemson for helping us to manage the *Millennium Simulation*, and Sandra Savaglio for her useful comments and suggestions. This work was partially supported by grants PICT 2005-32342, PICT 2006-245 Max Planck, and PICT 2006-2015 from Argentine ANPCyT.

## REFERENCES

- Bell E. F., McIntosh D. H., Katz N., Weinberg M. D., 2003, ApJS, 149, 289
- Bissaldi E., Calura F., Matteucci F., Longo F., Barbiellini G., 2007, A&A, 471, 585
- Bloom J. S., Djorgovski S. G., Kulkarni S. R., 2001, ApJ, 554, 678
- Bloom J. S., Berger E., Kulkarni S. R., Djorgovski S. G., Frail D. A., 2003, AJ, 125, 999
- Bornancini C. G., Martínez H. J., Lambas D. G., Le Floc'h E., Mirabel I. F., Minniti D., 2004, ApJ, 614, 84
- Campisi M. A., De Lucia G., Li L.-X., Mao S., Kang X., 2009, arXiv:0908.2427
- Castro Cerón J. M., Michalowski M. J., Hjorth J., Malesani D., Gorosabel J., Watson D., Fynbo J. P. U., 2008, arXiv:0803.2235
- Chabrier G., 2003, PASP, 115, 763
- Christensen L., Hjorth J., Gorosabel J., 2004, A&A, 425, 913
- Cole S., 1991, ApJ, 367, 45
- Courty S., Björnsson G., Gudmundsson E. H., 2004, MNRAS, 354, 581
- Daigne F., Rossi E. M., Mochkovitch R., 2006, MNRAS, 372, 1034
- De Lucia G., Blaizot J., 2007, MNRAS, 375, 2
- de Rossi M. E., Tissera P. B., De Lucia G., Kauffmann G., 2009, MNRAS, 395, 210
- Di Matteo P., Bournaud F., Martig M., Combes F., Melchior A.-L., Semelin B., 2008, A&A, 492, 31
- Frail D. A., Kulkarni S. R., Sari R. et al., 2001, ApJ, 562, L55
- Frontera F., Guidorzi C., Montanari E. et al., 2009, ApJS, 180, 192
- Fryer C. L., Woosley S. E., Hartmann, D. H., 1999, ApJ, 526, 152
- Fynbo J. P. U., Möller P., Thomsen B. et al. 2002, A&A, 388, 425

- Fynbo J. P. U., Jakobsson, P., Prochaska, J. X. et al. 2009, *ApJS*, 185, 526
- Galama T. J., Vreeswijk P. M., van Paradijs J. et al., 1998, *Nature*, 395, 670
- Glazebrook K., Abraham R. G., McCarthy P. J. et al. 2004, *Nature*, 430, 181
- Guetta D., Piran T. 2007, *JCAP*, 7, 3
- Hirschi R., Meynet G., Maeder A., 2005, *A&A*, 443, 581
- Hjorth J., Sollerman J., Møller P. et al., 2003, *Nature*, 423, 847
- Hurley K., Sommer M., Atteia, J.-L. et al., 1992, *A&AS*, 92, 401
- Jakobsson P., Björnsson G., Fynbo J. P. U. et al., 2005, *MNRAS*, 362, 245
- Katz N., Gunn J. E., 1991, *ApJ*, 377, 365
- Kauffmann G., White S. D. M., Heckman T. M., Ménard B., Brinchmann J., Charlot S., Tremonti C., Brinkmann J., 2004, *MNRAS*, 353, 713
- Kouveliotou C., Meegan C. A., Fishman G. J., Bhat N. P., Briggs M. S., Koshut T. M., Paciesas W. S., Pendleton G. N., 1993, *ApJ*, 413, L101
- Lacey C., Silk J., 1991, *ApJ*, 381, 14
- Lambas D. G., Tissera P. B., Alonso M. S., Coldwell G., 2003, *MNRAS*, 346, 1189
- Le Floc'h E., Duc P.-A., Mirabel I. F. et al., 2003, *A&A*, 400, 499
- MacFadyen A. I., Woosley S. E., 1999, *ApJ*, 524, 262
- Mészáros P., 2006, *Reports on Progress in Physics*, 69, 2259
- Metzger M. R., Djorgovski S. G., Kulkarni S. R., Steidel C. C., Adelberger K. L., Frail D. A., Costa E., Frontera F., 1997, *Nature*, 387, 878
- Modjaz M., Kewley L., Kirshner R. P. et al., 2008, *ApJ*, 135, 1136
- Mosconi M. B., Tissera P. B., Lambas D. G., Cora S. A., 2001, *MNRAS*, 325, 34
- Navarro J. F., White S. D. M., 1993, *MNRAS*, 265, 271
- Nuza S. E., Tissera P. B., Pellizza L. J., Lambas D. G., Scannapieco C., de Rossi M. E., 2007, *MNRAS*, 375, 665
- Panaiteescu A., Kumar P., 2001, *ApJ*, 560, L49
- Patton D. R., Grant J. K., Simard L., Pritchett C. J., Carlberg R. G., Borne K. D., 2005, *AJ*, 130, 2043
- Pélagneon A., Atteia J.-L., Nakagawa, Y. E. et al., 2008, *A&A*, 491, 157
- Perez M. J., Tissera P. B., Scannapieco C., Lambas D. G., de Rossi M. E., 2006, *A&A*, 459, 361
- Perez J., Tissera P., Blaizot J., 2009, *MNRAS*, 397, 748
- Poggianti B., Aragón-Salamanca A., Zaritsky D. et al., 2009, *ApJ*, 693, 112
- Pontzen A., Deason A., Governato F. et al., 2009, arXiv:0909.1321
- Prochaska J. X., Bloom J. S., Chen H.-W. et al., 2004, *ApJ*, 611, 200
- Salpeter E. E., 1955, *ApJ*, 121, 161
- Salvaterra R., Chincarini G., 2007, *ApJ*, 656, L49
- Sánchez A. G., Baugh C. M., Percival W. J., Peacock J. A., Padilla N. D., Cole S., Frenk C. S., Norberg P., 2006, *MNRAS*, 366, 189
- Savaglio S., 2006, *New Journal of Physics*, 8, 195
- Savaglio S., Glazebrook K., Le Borgne D., 2009, *ApJ*, 691, 182
- Scannapieco C., Tissera P. B., White S. D. M., Springel V., 2005, *MNRAS*, 364, 552
- Scannapieco C., Tissera P. B., White S. D. M., Springel V., 2006, *MNRAS*, 371, 1125
- Scannapieco C., Tissera P. B., White S. D. M., Springel V., 2008, *MNRAS*, 389, 1137
- Springel V., 2005, *MNRAS*, 364, 1105
- Springel V., Hernquist L., 2003, *MNRAS*, 339, 289
- Springel, V., White, S. D. M., Tormen, G., Kauffmann G., 2001, *MNRAS*, 328, 726
- Springel V., White S. D. M., Jenkins A. et al., 2005, *Nature*, 435, 629
- Stern B., Tikhomirova Y., Kompaneets D., Svensson R., Poutanen J., 2001, *ApJ*, 563, 80
- Thöne Ch. C., Fynbo, J. P. U., Östlin G. et al. 2008, *ApJ*, 676, 1151
- Wainwright C., Berger E., Penprase B. E., 2007, *ApJ*, 657, 367
- Wang J., De Lucia G., Kitzbichler M. G., White S. D. M., 2008, *MNRAS*, 384, 1301
- Weinmann S., van den Bosch F. C., Yang X., Mo H. J., 2006, *MNRAS*, 366, 2
- White S. D. M., Frenk C. S., 1991, *ApJ*, 379, 52
- Wijers R. A. M. J., Bloom, J. S., Bagla, J. S., Natarajan, P., 1998, *MNRAS*, 294, L13
- Wolf Ch., Podsiadlowski, Ph., 2007, *MNRAS*, 375, 1049
- Woosley S. E., 1993, *ApJ*, 405, 273
- Yoon S.-C., Langer N., Norman C., 2006, *A&A*, 460, 199
- Yonetoku D., Yamazaki R., Nakamura T., Murakami T., 2005, *MNRAS*, 362, 1114

This paper has been typeset from a Te<sub>X</sub>/ L<sub>a</sub>T<sub>e</sub>X file prepared by the author.